Neurobiology of Disease

Rescue of Infralimbic $mGluR_2$ Deficit Restores Control Over Drug-Seeking Behavior in Alcohol Dependence

Marcus W. Meinhardt,[1] Anita C. Hansson,[1] Stephanie Perreau-Lenz,[1] Christina Bauder-Wenz,[1] Oliver Stählin,[1] Markus Heilig,[2] Clive Harper,[3] Karla U. Drescher,[4] Rainer Spanagel,[1] and Wolfgang H. Sommer[1]

[1]Institute of Psychopharmacology at Central Institute of Mental Health, Medical Faculty Mannheim, University of Heidelberg, 68159 Mannheim, Germany, [2]Laboratory of Clinical and Translational Studies, National Institute on Alcohol Abuse and Alcoholism, National Institutes of Health, Bethesda, Maryland 20892, [3]New South Wales Tissue Resource Centre, University of Sydney, 2006 Sydney, Australia, and [4]Abbott Neuroscience Research, 67061 Ludwigshafen, Germany

A key deficit in alcohol dependence is disrupted prefrontal function leading to excessive alcohol seeking, but the molecular events underlying the emergence of addictive responses remain unknown. Here we show by convergent transcriptome analysis that the pyramidal neurons of the infralimbic cortex are particularly vulnerable for the long-term effects of chronic intermittent ethanol intoxication. These neurons exhibit a pronounced deficit in metabotropic glutamate receptor subtype 2 ($mGluR_2$). Also, alcohol-dependent rats do not respond to $mGluR_{2/3}$ agonist treatment with reducing extracellular glutamate levels in the nucleus accumbens. Together these data imply a loss of autoreceptor feedback control. Alcohol-dependent rats show escalation of ethanol seeking, which was abolished by restoring $mGluR_2$ expression in the infralimbic cortex via viral-mediated gene transfer. Human anterior cingulate cortex from alcoholic patients shows a significant reduction in $mGluR_2$ transcripts compared to control subjects, suggesting that $mGluR_2$ loss in the rodent and human corticoaccumbal neurocircuitry may be a major consequence of alcohol dependence and a key pathophysiological mechanism mediating increased propensity to relapse. Normalization of $mGluR_2$ function within this brain circuit may be of therapeutic value.

Introduction

The molecular and neuroanatomical substrates underlying substance use disorders including alcohol dependence remain poorly understood. Imbalances in glutamate neurotransmission and homeostasis are considered to play a central role for the increased propensity to relapse in addicted individuals (Everitt and Robbins, 2005; Kalivas, 2009; Spanagel, 2009). In particular, the glutamatergic corticoaccumbal pathway plays an essential role for reinstating drug-seeking behavior in animal models of relapse (Kalivas, 2009). It has been shown that lesions or inactivation of the medial prefrontal cortex (mPFC) or nucleus accumbens prevent reinstatement of drug seeking following extinction, while activation of either structure stimulates drug seeking (Cornish and Kalivas, 2000; Capriles et al., 2003; McFarland et al., 2004). Supporting this notion, human functional magnetic resonance imaging identified a positive correlation between cue reactivity, craving, and activity in prefrontocortical regions in addicted patients (Wilson et al., 2004; Schacht et al., 2013). A dysregulation of central glutamate levels in these areas during withdrawal and protracted abstinence was recently reported as well (Hermann et al., 2012a,b). Despite these findings on the role of the mPFC–accumbal pathway in relapse, relatively little is known about the molecular and cellular neuroadaptations within this circuit that result in susceptibility to relapse.

Here we set out to elucidate alcohol-induced dysregulation of mPFC function in rats with a history of alcohol dependence, i.e., by exposure to daily cycles of intermittent alcohol vapor intoxication and withdrawal, a paradigm that produces high intoxication with brain alcohol levels above 200 mg/dl and induces behavioral and molecular changes relevant for the pathophysiology of alcoholism in both rats and mice (Rogers et al., 1979; Roberts et al., 2000; Rimondini et al., 2002, 2003, 2008; Becker and Lopez, 2004; O'Dell et al., 2004; Hansson et al., 2008; Sommer et al., 2008; Melendez et al., 2012). Animals derived from this procedure are termed "postdependent" to emphasize the fact that neuroadaptations induced through a history of alcohol dependence remain even in the absence of continued ethanol intoxication. This phenomenon has been consistently demonstrated for a long-lasting behavioral sensitivity to stress and altered amygdala (Amy) gene expression (Funk et al., 2006; Heilig and Koob, 2007; Sommer et al., 2008; Vendruscolo et al., 2012). In this sense, postdependent animals may model the increased propensity to relapse in abstinent alcoholic patients (Björk et al., 2010; Heilig et al., 2010). We used a multilayered search strategy

Received Aug. 23, 2012; revised Oct. 19, 2012; accepted Oct. 29, 2012.

Author contributions: M.W.M., A.C.H., S.P.-L., M.H., R.S., and W.H.S. designed research; M.W.M., A.C.H., S.P.-L., C.B.-W. O.S., K.U.D., and W.H.S. performed research; M.H., C.H., and K.U.D. contributed unpublished reagents/analytic tools; M.W.M., M.H., K.U.D., R.S., and W.H.S. analyzed data; M.W.M., R.S., and W.H.S. wrote the paper.

This work was supported by the Bundesministerium für Bildung und Forschung within the frameworks of NGFN Plus (FKZ 01GS08151, 01GS08152, and 01GS08155; see www.ngfn-alkohol.de, Spanagel et al., 2010) and ERA-Net TRANSALC (FKZ 01EW1112), the European Commission FP-6 Integrated Project IMAGEN (PL037286), the Deutsche Forschungsgemeinschaft (Center Grant SFB636; project Grant HA 6102/1-1 to A.C.H.; Reinhart-Koselleck Award SP 383/5-1 to R.S.), and the Intramural Research Program of the NIAAA (M.H.). We thank Elisabeth Röbel and Fernando Leonardi-Essmann for assistance in laboratory experiments.

The authors declare no competing financial interests.

Correspondence should be addressed to Wolfgang H. Sommer, Central Institute of Mental Health, Square J5, 68159 Mannheim, Germany. E-mail: wolfgang.sommer@zi-mannheim.de.

DOI:10.1523/JNEUROSCI.4062-12.2013

 0270-6474/13/332794-13$15.00/0

that started with an unbiased transcriptome screening of multiple brain regions and converged on a distinct neuronal population that exhibits a profound metabotropic glutamate receptor subtype 2 ($mGluR_2$) deficit. This receptor belongs to the Class II metabotropic glutamate receptors ($mGluR_{2/3}$) that are key to regulating glutamatergic neurotransmission in brain regions mediating drug seeking and incentive motivation, including the mPFC–accumbal pathway (Ohishi et al., 1993; Olive, 2009). $mGluR_{2/3}$ negatively modulate glutamate transmission as autoreceptors by inhibiting glutamate release and by reducing neuronal excitability at the postsynaptic level (Ferraguti and Shigemoto, 2006). Dysregulation of $mGluR_{2/3}$ function within the mPFC–accumbal pathway has been found after withdrawal from chronic exposure to cocaine, nicotine, and opioids (Liechti and Markou, 2007; Moussawi et al., 2009; Olive, 2009). Here we found that the $mGluR_2$ autoreceptor function is specifically disrupted after a history of alcohol dependence, which allowed us to develop a rescue strategy for restoring behavioral control in alcohol-dependent rats by focal $mGluR_2$ overexpression.

Materials and Methods

Animal husbandry. Male Wistar rats, initial weight 220–250 g, were used (Charles River), housed four per cage under a 12 h light/dark cycle with *ad libitum* access to food and water. All behavioral testing was performed during the dark phase, 5 d per week. All experiments were conducted in accordance with the ethical guidelines for the care and use of laboratory animals and were approved by the local animal care committee (Regierungspraesidium Karlsruhe, Karlsruhe, Germany). Five batches of animals were uniformly treated with either intermittent alcohol vapor or air exposure: Batch 1, $n = 10$ per group for microarray and $n = 8$ per group for *in situ* hybridization; Batch 2, $n = 8$ per group for laser-capture microscopy (LCM) study; Batch 3, $n = 8$ per group for microdialysis; Batches 4 and 5, $n = 8$ and 16 per group for operant self-administration experiments, respectively.

Ethanol exposure. Rats were weight-matched, assigned into the two experimental groups, and exposed to either ethanol vapor or normal air using a rodent alcohol inhalation system as described previously (Rimondini et al., 2002). Briefly, pumps (Knauer) delivered alcohol into electrically heated stainless-steel coils (60°C) connected to an airflow of 18 L/min into glass and steel chambers ($1 \times 1 \times 1$ m). For the next 7 weeks rats were exposed to five cycles of 14 h of ethanol vapor per week (0:00 A.M. to 2:00 P.M.) separated by daily 10 h periods of withdrawal. Twice per week, blood ($\sim$20 μl) was sampled from the lateral tail vein, and blood alcohol concentrations were determined using an AM1 Analox system (Analox Instruments). After the last exposure cycle, rats remained abstinent for 2–3 weeks before further entering further experiments (3 weeks for gene expression and microdialysis analysis, 2 weeks for resumption of operant training).

Measurement of ethanol withdrawal signs. Using a withdrawal rating scale according to Macey et al. (1996), alcohol withdrawal signs including irritability to touch (vocalization), body tremors, tail rigidity, and ventromedial limb retraction were weekly scored, 6 h after ethanol vapor was turned off. Each sign was assigned a score of 0–2, based on the following severity scale: 0, no sign; 1, moderate; 2, severe. The sum of the four observation scores (0 to 8) was used as a quantitative measure of withdrawal severity. For these behavioral observations, animals were individually transferred from their home cages to a quiet observation room to avoid extraneous stimulation, and animals were observed in a blind fashion.

Rat brain tissue samples and microarray experiment. Three weeks after the last exposure cycle, postdependent (alcohol exposed, $n = 10$) and control (air exposed, $n = 10$) animals were killed during the first 4 h of the light cycle by decapitation, and brains were frozen in −40°C isopentane and kept at −80°C. Bilateral samples were obtained under a magnifying lens using anatomical landmarks (Paxinos and Watson, 1998). Amygdala, nucleus accumbens, and medial prefrontal cortex including Cg1 + 2, prelimbic cortex, and infralimbic cortex) according to Paxinos and Watson (1998) were prepared as described previously (Arlinde et al., 2004). Briefly, amygdala was prepared from a 2 mm-thick-coronal slice, taken in a Kopf brain slicer by placing the rostral blade on the caudal edge of the optic chiasm. For preparation of cingulate cortex and accumbens, the rostral blade was placed 4 mm rostral to this landmark, and a second 2 mm coronal slice was obtained. Cortical tissue was dissected out with a scalpel, while amygdala and accumbens tissues were obtained using a punch (2 mm diameter). Samples were stored at −80°C until RNA was prepared.

Total RNA was extracted with Trizol reagent (Invitrogen) followed by an RNeasy (Qiagen) column-based cleanup step according to the manufacturer's instructions. All RNA samples showed A260/280 absorption ratios between 1.9 and 2.1. RNA integrity was determined using an Agilent 2100 Bioanalyzer (Agilent Technologies), and only material without signs of degradation was used.

Microarray target preparation was done for individual samples and hybridization to RAE230A arrays, staining, washing, and scanning of the chips were performed according to the manufacturer's technical manual (Affymetrix). The Microarray Analysis Suite 5.0 (MAS5)-produced CEL files were inspected for regional hybridization bias and quality control parameters as described previously (Reimers et al., 2005). Forty-eight microarrays (mPFC, 9 and 9; accumbens, 7 and 7; amygdala, 7 and 9, postdependent and control rats, respectively) passed quality control. The MAS5 recognized $\sim$60% of the 15 800 probe sets on the RAE230A array as present in our samples. Robust multichip average expression values were obtained and tested for differential gene expression using Welch's two-sample t test, assuming unequal variances at a $p < 0.05$ threshold. The microarray CEL files were imported into gene set enrichment analysis (GSEA) software, available at www.broadinstitute.org/gsea/, and gene set enrichment analysis was performed against gene sets for glutamatergic and GABAergic neurons described by Sugino et al. (2006) (Table 1).

Human brain tissue. Human brain tissue samples were obtained from the New South Wales Tissue Resource Centre at the University of Sydney, Australia (http://www.pathology.usyd.edu.au/trc.htm). Tissue from 30 male subjects of European descent consisting of 15 chronic alcoholics

Table 1. Gene sets for glutamatergic and GABAergic neurons

Glutamatergic genes		GABAergic genes
Adora1	*Kpna1*	*Abat*
Ak3l1	***Lmo4***	*Capza1*
Ap1gbp1	*Lmo7*	*Cds2*
Arpc5	*Mast3*	*Cygb*
Arpp21	*Neurod2*	*Gad1*
Baiap2	*Nphp1*	*Gad2*
Cpd	*Nrgn*	*Grik1*
Crip2	***Nupl1***	*Kcnc1*
Crym	*Ppp3ca*	*Klhl13*
Dgat2	***Ptk2***	*Ltbp3*
Dusp14	*Ptk2b*	*Map3k1*
Egr4	*Rap2b*	*Paip2*
Ensa	*Rin1*	*Pcaf*
Ets2	*Srr*	*Pcp4l1*
Fhl2	*St3gal5*	*Pdxk*
Galntl1	***Stx1a***	*Ppp3cb*
Gpm6b	*Synpo*	*Ptprm*
Gria2	*Tesc*	*Rpp25*
Hebp1	*Tjp1*	*Slc32a1*
Igfbp6	***Tyro3***	*Slc6a1*
Itpka	*Zfp179*	*Socs5*
Klf10	*Zfp238*	*Sv2a*
Klhl2		*Txnl1*

Gene sets were taken from Sugino et al. (2006) who found extremely divergent expression profiles from GABA-ergic interneurons and glutamatergic pyramidal neurons. p values for top candidates ranged from a maximum of 1.5×10^{-11} to 1.8×10^{-27} (GABAergic versus glutamatergic population). Only genes that had rat homologes and were present on the Affymetrics arrays were used. Significant genes in the microarray experiment from mPFC are in bold letters.

Table 2. Primer sequences used of QRT-PCR

Species	Name	RefSeq ID	Forward primer	Reverse primer
Rat	*Actb*	NM_031144.2	AGCCATGTACGTAGCCATCCA	TCTCCGGAGTCCATCACAATG
Rat	*Crym*	NM_053955	CATCTGGCAAGTGAGCAGAA	GGGACTAGGCCTCCTTTGAT
Rat	*Egr1*	NM_012551.2	CAGGAGTGATGAACGCAAGA	GGGATGGGTAGGAAGAGAGG
Rat	*Egr2*	NM_053633	TCCGAGTTCTGAACCTTTGG	GGACACTTGCAACACCACTG
Rat	*Egr4*	NM_019137.1	CACAGAGCAGGCGATACCTT	ACATCCCCAGCTTGACTCTG
Rat	*Grm2*	NM_001105711.1	GTGAGGTGGTGGACTCAACA	CGTGGATGAGGGTCTATGCT
Rat	*Gria3*	NM_032990.2	ACTGAAAACGTGGCTGCTTC	GAAAGGTCATTGCACCATCA
Rat	*Nr4a1*	NM_024388.1	CCTCATTCCAGAAGATGGACA	TGAGCTGGGAGGGATAAGAG
Rat	*Nr4a3*	NM_017352	TACGGAGTCCGCACCTGCGA	CGACGTCTCTTGTCTACCGGGC
Rat	*Slc1a3*	NM_019225.1	TGGGCCTGCCCACGGATGA	CCCGGCCCCGAGGGAG
Human	*Gapdh*	NM_002046.4	CATGAGAAGTATGACAACAGCCT	AGTCCTTCCACGATACCAAAGT
Human	*Grm2*	NM_001130063.1	CGCCGCCTCTACAAGGACT	GGCCAATACCATCACCAAAG

and 15 control cases was used for this study. Subject affiliation to the alcoholics or control group was confirmed postmortem using the Diagnostic Instrument for Brain Studies–Revised, which is consistent with the criteria of the *Diagnostic and Statistical Manual for Mental Disorders*, fourth edition (DSM-IV) (American Psychiatric Association, 1994). All alcoholics had consumed >80 g of ethanol per day, whereas the control cases had an average daily consumption of <20 g. To reduce the number of confounding factors, we tried to not include any subjects where the cause of death was suicide, the postmortem interval was >40 h, or blood alcohol or significant amounts of psychiatric medication (concentration >1.0 mg/L) was detected at the autopsy whenever possible. For each subject, we analyzed tissue samples from the anterior cingulate cortex.

RNA extraction and analysis was done as described previously (Sommer et al., 2010). RNA from brain tissue was isolated using Trizol according to manufacturer's protocol (Invitrogen). RNA samples underwent a cleanup step using the RNeasy Mini Kit (Qiagen) and were then treated with RQ1 RNase-free DNase (Promega) following manufacturer's instructions, to eliminate DNA contamination. All RNA samples had acceptable 260/280 ratios (1.8–2.1). RNA samples were then analyzed with an Agilent 2100 Bioanalyzer and the RNA integrity number. RNA (100 ng) was used for cDNA synthesis using reverse transcription reagents according to the manufacturer's protocol (Applied Biosystems). For the quantitative real-time (qRT)-PCR method, see below, Quantitative RT-PCR from micropunched, amplified, and human tissue. In addition to *GAPDH*, we used *ALUSX* as a second endogenous control. Results were similar for both reference genes.

Stereotaxic injections. For stereotaxic injections of the retrograde tracer ($n = 8$ per group), rats were anesthetized (isofluran) and placed in a Kopf stereotaxic instrument, and 300 nl of rhodamine-labeled fluorescent latex microspheres (Lumafluor) were delivered to the nucleus accumbens shell at 70 nl/min using a WPI microinjectionpump through a 33 gauge beveled needle. The stereotaxic coordinates for the injections (Wistar rats, 500 g) were +1.8 mm AP, +0.9 mm ML, and −7.5 mm DV relative to bregma. Following surgery, rats were single housed for 2 d. After a 7 d recovery period, rats were euthanized for tissue collection as described below.

For lentiviral injections, rats received 600 nl of either Lenti-control or Lenti-mGluR$_2$ to bilaterally into the infralimbic cortex at 70 nl/min. The stereotaxic coordinates for the injections (500 g Wistar rats) were +3.2 mm AP, ±0.52 mm ML, and −5.1 mm DV relative to bregma.

Gene expression analysis of infralimbic projection neurons via qRT-PCR. Rats recovered for 1 week following stereotaxic tracer delivery. For perfusions, rats were anesthetized (ketamin/xylazin, 100/5 mg/kg, i.p.) and transcardially perfused with ice-cold 50 ml PBS followed by 80 ml 0.5% paraformaldehyde (PFA) containing 20% sucrose. After perfusions, brains were removed and flash frozen in −40°C isopentanol and stored at −80°C up to 72 h before sectioning.

Frozen brains were cut into 12-μm-thick coronal sections with a cryostat. Sections were mounted on PALM membrane slides and kept at −80°C and process at the same day. Just before LCM, slides were thawed to −25°C; rapidly trimmed of tissue tech; dehydrated with 75% EtOH (30s), 95% EtOH (30s), 100% EtOH (30s), and xylene (1 min); and then air-dried for 5 min and immediately used for LCM.

LCM was performed using a Zeiss PALM laser system. Tracer-labeled cells were identified using a CY3 advanced filter cube (excitation, bandpass 546/12; emission, bandpass 575–640). The laser focus followed a circular trajectory of 8–10 μm in diameter to cut out and separate tracer positive cells from the adjacent tissue, following a final slightly subfocal laser pulse to catapult the cell into an LCM cup. Laser-targeted cells were bonded to adhesive LCM caps by aiming the laser beam at the thin plastic sheet in the cap directly above the target cell. Per animal, ~70–100 cells were collected.

RNA was extracted with the RNeasy Micro kit for microdissected cryosections. All steps were performed according to the manufactures recommendations. A speed vac (Vacufuge 2015727; Eppendorf) was used to dry down the eluted RNA to 3 μl for the further amplification step. Total RNA was amplified using the TargetAmp 2-Round aRNA Amplification Kit 2.0 (Epicenter) according to manufacturer's recommendations. We typically obtained 2–5 μg of amplified RNA after the second amplification round. Amplifications were performed from six exposed and seven control tracer cell RNA extractions.

Quantitative RT-PCR from micropunched, amplified, and human tissue. RNA (100 ng total) was reverse transcribed using the High Capacity RNA-to-cDNA Master Mix (Applied Biosystems) following the manufacturer's protocol. Samples were assayed in triplicate in a total reaction volume of 20 μl using Power SYBR Green PCR Master Mix (Applied Biosystems) on an Applied Biosystems 7900 HT RT-PCR System (40 cycles of 95°C for 15 s and 60°C for 1 min). A melting profile was recorded at the end of each PCR to check for aberrant fragment amplifications. Primers for each target were designed toward the 3′ end of the coding sequence by considering exon–exon junctions when possible, based on the National Center for Biotechnology Information reference sequence database. Amplicons were designed with 95–110 bp length and melting temperatures >75°C to be able to distinguish between amplicons and primer-dimer formations in the melting analysis. For primer sequences, see Table 2. The Applied Biosystems SDS 2.2.2 software was used to analyze the SYBR Green fluorescence intensity and to calculate the theoretical cycle number when a defined fluorescence threshold was passed (Ct values). Relative quantification was done according to the 2-ΔΔCT method, whereby Actin β (Actb) was used as internal normalizer for rat tissue and glyceraldehyde-3-phosphate dehydrogenase (GAPDH) for the human tissue. The 2-ΔΔCt method is defined such that a cycle (Ct) is the cycle at which there is a significant detectable increase in fluorescence; the ΔCt value is calculated by subtracting the Ct value for the endogenous control from the Ct value for the mRNA of interest. The ΔΔCt value is calculated by subtracting the ΔCt value of the control sample from the ΔCt of the experimental sample. For graphical interpretation, the ΔΔCt values were transformed ($-x$); thus downregulated genes show ΔΔCt values <0 and upregulated genes show ΔΔCt values >0. The −ΔΔCt values were compared by an unpaired t test for each gene ($p < 0.05$ considered significant). Actb and GAPDH Ct values were not different between groups. Statistical testing was done by t test on the ΔΔCT values. The software and ΔΔCT method was used to determine statistical significance. Melting curves for all primers used in this study exhibited single fluorescence change peaks at the appropriate melting temperatures. This indicates the absence of primer-dimer formation.

In situ hybridization. Riboprobes and *in situ* hybridizations were performed as described previously (Hansson et al., 2008). In a parallel batch of animals to the microarray, postdependent (alcohol exposed, $n = 8$) and control (air exposed, $n = 8$) animals were killed by decapitation during the first 4 h of the light phase, and brains were frozen in −40°C isopentane and kept at −80°C. Coronal brain sections (10 μm) were cryosectioned at forebrain bregma levels +3.0 mm and +2.0 mm. The rat-specific riboprobes for all genes were generated based on the gene reference sequence in the PubMed database (http://www.ncbi.nlm.nih.gov/Entrez): Egr-1, position 1384 to 1851 bp on rat cDNA (gene reference number, NM_012551.1); $mGluR_2$, position 1327 to 1620 bp on rat cDNA (gene reference number, XM_343470.1); $mGluR_3$, position 314 to 662 bp on rat cDNA (gene reference number, XM_342626.1); NMDA receptor 2a, position 434 to 876 bp on rat cDNA (gene reference number, RATNMDA2A); NMDA receptor 2b, position 205 to 591 bp on rat cDNA (gene reference number, NM_012574.1).

Phosphor imager-generated (Fujifilm Bio-Imaging Analyzer Systems) digital images were analyzed using MCID Image Analysis Software (Imaging Research). Regions of interest were defined by anatomical landmarks as described in the atlas of Paxinos and Watson (1998) and illustrated in Figure 2. Based on the known radioactivity in the 14C standards, image values were converted to nanocuries per gram.

Microdialysis and assay of microdialysate glutamate levels. Three weeks after ethanol exposure, rats weighed 450–550 g for surgery and were housed in groups of four before and individually after surgery. Rats were anesthetized (isofluran, 1.5–2%) and placed in a stereotaxic frame (Kopf Instruments). CMA11 guide cannula (20 gauge, 14 mm; CMA Microdialysis) were unilaterally implanted 2.0 mm above the nucleus accumbens shell (+1.6 mm AP, ±0.8 mm ML, and 5.6 mm DV). Coordinates were based on bregma, midline, and dura, respectively (Paxinos and Watson, 1998). Cannulas were anchored with three stainless-steel screws and dental acrylic. Animals were allowed to recover from surgery for 1 week.

Microdialysis experiments were conducted in conscious, freely moving rats, 3 weeks after last ethanol vapor exposure. Dialysis probes (CMA11 2 mm; CMA Microdialysis) with 2 mm active membrane were introduced into the guide cannula 12 h before the beginning of the dialysis experiments to minimize damage-induced release of neurotransmitters and metabolites. Each animal participated in one only microdialysis experiment. Samples were collected every 15 min at a flow rate of 1.5 μl/min. After 3 baseline samples, rats were injected with a saline solution as a control. Thirty minutes later rats were injected intraperitoneally with 3 mg/kg $mGluR_{2/3}$ agonist LY379268 ((1R,4R,5S,6R)-4-amino-2-oxabicyclo[3.1.0]hexane-4,6-dicarboxylic acid), and sampling continued for the remaining time of the experiment.

Eight microliters of ortho-pthaldialdehyde/*N*-isobutyryl-L-cysteine solution (from Calbiochem and Fluka, respectively) were added to 20 μl microdialysate or standard volume. After three times mixing and a reaction time of 3 min, 14 μl were injected (CTC PAL autosampler; Axel Semrau) onto a HPLC column (Waters Xbridge C18 3.5 μm 10/2.1 mm guard cartridge and Waters Xbridge C18 3.5 μm 100/2.1 mm). The mobile phase consisted of 50 mM Na_2HPO_4, 1 mM Na-EDTA, 20% methanol, pH 6.5, with phosphoric acid. Flow rate was set to 0.3 ml/min (Rheos flux pump; Axel Semrau). Between every single injection, the system was flushed with 20 μl acetonitrile. Glutamate was measured via a fluorescence detector (L-7480; Merck). The system was calibrated by standard solutions of glutamate containing 10 pmol/10 μl per injection. Glutamate was identified by its retention time and peak height with an external standard method using chromatography software (Chrom Perfect; Justice Laboratory Software).

Immunohistochemistry. Rats were killed by transcardial perfusion with 0.9% saline (w/v) followed by 4% PFA (w/v) in 1× PBS. Brains were postfixed in 4% buffered PFA at 4°C for 12 h, dehydrated in 1× PBS-sucrose (10%) solution for 3–7 d, and flash frozen at −80°C. Sections (14 μm) were cut with a cryostat, cycled with an ImmunoPen, washed one time for 5 min (200 μl of 0.01 M PBS, pH 7.4 on the sections), and air dried. Sections were incubated with primary antibody in diluted 0.01 M PBS, pH 7.4, plus 0.3% Triton X-100 at 4°C overnight, followed by appropriate secondary antibodies (diluted with 0.01 M PBS, pH 7.4, plus 0.03% Triton X-100) for 1 h at room temperature. All antibodies were tested for optimal dilution, the absence of cross-reactivity, and nonspecific staining. To detect the enhanced GFP, we used rabbit eGFP, diluted 1:500 (Invitrogen), as primary antibody and donkey-anti-rabbit Alexa 488, diluted 1:600 (Invitrogen), as secondary antibody. For visualization of the $mGluR_2$ we used a mouse-$mGluR_2$, diluted 1:500 (Santa Cruz Biotechnology), as primary antibody and the donkey-anti-mouse 594, diluted 1:800 (Invitrogen), as secondary antibody.

Operant alcohol self-administration apparatus. All alcohol-seeking experiments were performed in operant chambers (MED Associates) enclosed in ventilated sound-attenuating cubicles. The chambers were equipped with a response lever on each side panel of the chamber. Responses at the appropriate lever activated a syringe pump that delivered a ~30 μl drop of fluid into a liquid receptacle next to it. A light stimulus (house light) was mounted above the right response lever of the self-administration chamber. An IBM-compatible computer controlled the delivery of fluids, presentation of stimuli, and data recording.

The reinstatement protocol used in the present report is the one that was used by Ciccocioppo et al. (2002) with a slight modification, i.e., a syringe pump delivered a ~30 μl drop of fluid into a liquid receptacle as opposed to 100 μl drop of fluid in the Ciccocioppo protocol. This modification markedly increased responding for alcohol (approximately fivefold), which allowed us to better monitor animals' motivation to receive alcohol.

Alcohol self-administration training. All animal training and testing sessions were performed during the dark phase of their light cycle. Animals were trained to self-administer 10% (v/v) ethanol in daily 30 min sessions using a fixed-ratio 1 (FR1) schedule using Samson's sucrose-fading procedure (Tolliver et al., 1988). During the first 3 d of training, animals were kept fluid deprived for 20 h per day. Responses at the left lever were reinforced by the delivery of 0.2% (w/v) saccharin solution. For the next 3 d, animals underwent the same procedure without fluid deprivation. Following acquisition of saccharin-reinforced responding, rats were trained to self-administer ethanol. During the next three sessions, responses at the left lever resulted in the delivery of 0.03 ml of 5% (v/v) ethanol plus 0.2% saccharin solution. Responses at the left lever were recorded but had no programmed consequences. Thereafter, the concentration of ethanol was increased first to 8% and then to 10% v/v, and the concentration of saccharin was decreased until saccharin was eliminated completely from the drinking solution.

Conditioning phase. The purpose of the conditioning phase was to train the animals to associate the availability of ethanol with the presence of specific discriminative stimuli. This phase started after the completion of the saccharin-fading procedure. Discriminative stimuli predicting ethanol (10%) availability were presented during each subsequent daily 30 min session. An orange flavor extract served as the cue stimulus for ethanol. This olfactory stimulus was generated by depositing six drops of an orange extract into the bedding of the operant chamber before each session. In addition, each lever press resulting in ethanol delivery was accompanied by a 5 s blinking conditioned light stimulus (CS). The 5 s period served as a "time-out," during which responses were recorded but not reinforced. At the end of each session, the bedding of the chamber was changed, and trays were thoroughly cleaned. The animals received a total of 10 ethanol conditioning sessions. Throughout the conditioning phase, responses at the right lever were recorded but not reinforced (inactive lever). After the final conditioning phase, rats were sorted into two balanced experimental groups of which one was exposed to alcohol vapor (resulting in the postdependent group) and the other received normal air (control group).

Conditioning and extinction phase in postdependent rats. Following a 2 week abstinence phase, all animals were reconditioned to self-administer 10% ethanol in 10 daily conditioning sessions. After completing the reconditioning phase, rats were subjected to daily 30 min extinction sessions for 12 consecutive days, which in total were sufficient to reach the extinction criterion of <10 lever responses per session. Extinction sessions began by extending the levers without presenting olfactory discriminative stimuli. Responses at the previously active lever activated the syringe pump, without resulting in the delivery of ethanol or the presentation of response-contingent cues (stimulus light).

Reinstatement testing. For reinstatement, animals were divided into two groups per condition (control and postdependent) on the basis of their

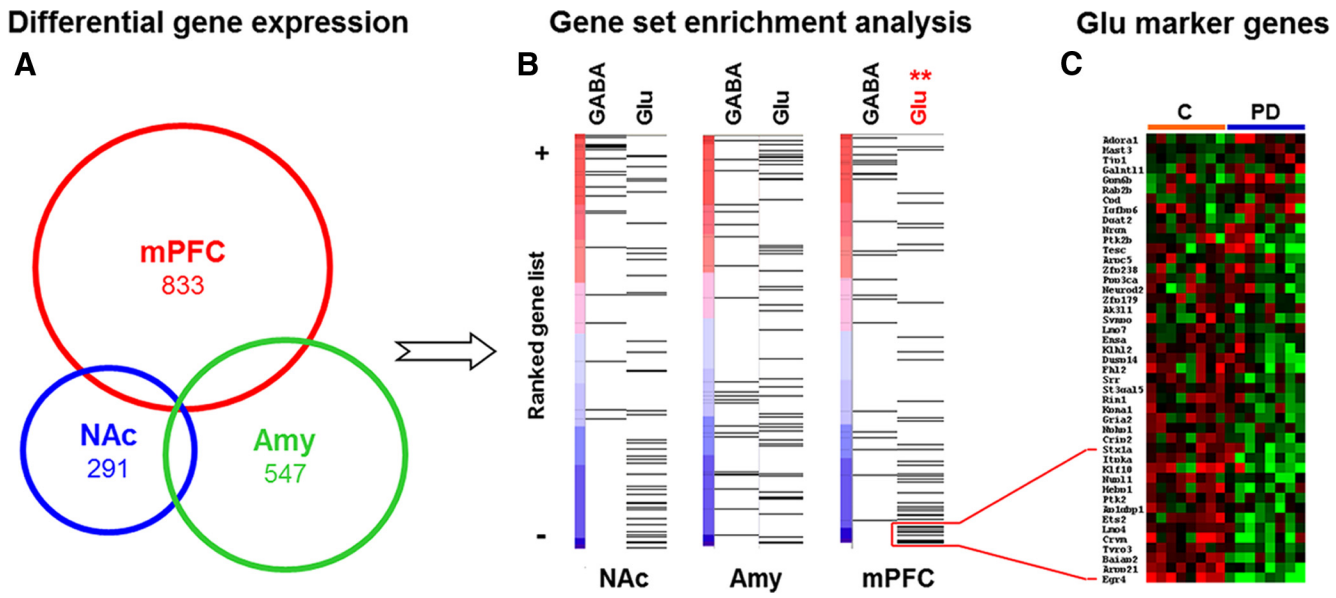

Figure 1. Expression analysis from three brain regions of postdependent (PD) rats and controls showing a distinct downregulation of glutamatergic marker genes in mPFC. Samples from mPFC, nucleus accumbens (NAc), and Amy of postdependent rats and controls were processed on Affymetrix GeneChip arrays. ***A***, Venn diagram showing the number of significant differently expressed genes in each region. ***B***, GSEA shows significant downregulation of an a priori defined set of glutamatergic marker genes in the mPFC, but not in the other regions. Each line corresponds to a gene of the respective set and is positioned according to its ranked effect size among all analyzed genes on the microarray (for gene sets, see Table 1). NAc-GABA, Normalized enrichments score, 1.4159; nominal p value, 0.0819; false discovery rate (FDR) q value, 0.1082; NAc-GLU, normalized enrichments score, −1.2078; nominal p value, 0.2218; FDR q value, 0.2596; Amy-GABA, normalized enrichments score, −0.6877; nominal p value, 0.8511; FDR q value, 0.8632; Amy-GLU, normalized enrichments score, 0.9564; nominal p value, 0.4991; FDR q value, 0.5629; mPFC-GABA, normalized enrichments score, 1.4622; nominal p value, 0.0489; FDR q value, 0.1259; mPFC-GLU, normalized enrichments score, −1.6227; nominal p value, 0.0; FDR q value, 0.0021. **$p < 0.01$ (corrected). ***C***, Heat map showing the expression of the glutamatergic marker genes postdependent and control rats. Thirteen of 45 genes of the set are significantly downregulated in postdependent rats ($p < 0.05$). Red shows higher and green shows lower expression compared to the mean of all samples.

performance during the last four retraining sessions. After the last extinction trial, animals received bilateral stereotaxic injections in the infralimbic cortex (for details, see above, Stereotaxic injections). Reinstatement began 7 d after the final extinction session. In these tests, rats were exposed to the same conditions as during the conditioning phase, except that the ethanol was not available. Sessions were initiated by the extension of both ethanol-associated and inactive levers and the presentation of the discriminative stimulus predicting ethanol. Responses at the ethanol-associated lever were followed by the activation of the syringe pump without any ethanol delivery and the presentation of the CS (light).

Generation of Lenti-mGluR$_2$ vector. The mGluR$_2$ cDNA was amplified using the IMAGp998E1215366Q clone as a template (Imagenes). After purification, the cDNA was cloned into the pCDH-MCS-T2A-copGFP vector (BioCat). The vector containing the mGluR2 insert was purified, sequenced, tested in cell culture, and finally used for lentiviral production. Active lentiviral particles were produced by System Biosciences.

Statistics. Microarray, PCR and *in situ* hybridization data were compared by t test. Data from the microdialysis experiment were analyzed using two-way repeated-measures ANOVA. Behavioral experiments were analyzed by two-way ANOVA or t test where appropriate. *Post hoc* testing was done with Fisher LSD test. The withdrawal scores were compared using a Mann–Whitney test. Statistical significance was set at a $p < 0.05$. Statistica 10.0 software for Windows was used (StatSoft).

Results

Gene expression analysis in ethanol responsive brain regions point to the infralimbic region

We started with an unbiased transcriptome analysis to determine potential targets of alcohol-induced neuroadaptations, classified the affected cell types in the region, and identified candidate genes for further experiments. Microarray-based transcriptome analysis revealed that chronic intermittent alcohol exposure had long-term effects on gene expression in three brain regions implicated in drug dependence, namely, mPFC, nucleus accumbens, and amygdala (Koob and Volkow, 2010) (Fig. 1*A*). We used GSEA (Subramanian et al., 2005) to test the hypothesis of functionally related postdependent neuroadaptations in GABAergic or glutamatergic neurons. For this purpose, we used two marker gene sets described previously as extremely divergent between GABAergic and glutamatergic neurons (Sugino et al., 2006). Results indicate a highly significant enrichment of downregulated glutamatergic marker genes ($p < 0.01$) in the mPFC of postdependent rats (Fig. 1*B*,*C*; Table 1). We selected a number of candidate genes for corroborative analysis by quantitative PCR (Table 3). Among the confirmed candidates was *Grm2*, the gene coding for mGluR$_2$, which was robustly downregulated in the mPFC of postdependent rats compared to controls. We next used *in situ* hybridization to address the question whether or not a specific subregion of the mPFC is preferentially affected in postdependent rats. Several genes derived from the transcriptome study, i.e., members of the activity-dependent Egr-family (*Egr1* and *Egr2*) and glutamate receptors (*Nr-2a*, *Nr-2b*, *Grm2*) showed significant downregulation only in the infralimbic cortex, with the most profound effect again the gene for mGluR$_2$ (Fig. 2*A*,*B*). In contrast, the expression of the pharmacologically highly similar mGluR$_3$ was not altered in this region (mean nanocuries per grams ± SEM; infralimbic cortex, control, 40.80 ± 2.13; postdependent, 41.59 ± 2.19; not significant; prelimbic cortex, control, 51.49 ± 1.75; postdependent, 53.06 ± 1.09; not significant). Together, these findings suggest that the infralimbic cortex is a hot spot within the mPFC for alcohol dependence-induced alterations.

Infralimbic–accumbal glutamatergic projection neurons are highly sensitive to alcohol dependence-induced neuroadaptations

Together, these experiments lead to the conclusion that glutamatergic neurons in the infralimbic cortex are highly sensitive to alcohol-induced neuroplasticity. To identify the specific neuro-

Table 3. QRT-PCR validation of selected candidate genes from micropunched tissue and IL projection neurons cells

		Microarray bulk		qRT-PCR bulk		qRT-PCR IL neurons	
Gene	Gene title	*p*	FC	*p*	FC	*p*	FC
Egr1	Early growth response 1	0.0231	−0.2524	**0.0137**	**−0.5738**	0.196	−1.294
Egr2	Early growth response 2	0.0084	−0.7276	**0.0123**	**−0.8669**	**0.006**	−9.844
Egr4	Early growth response 4	0.0006	−0.5907	**0.0077**	**−0.7916**	**0.041**	−1.203
Gria3	Ionotrophic glutamate receptor 3	0.0356	−0.3008	**0.0368**	**−0.3686**	0.683	−0.316
Grm2	Metabotropic glutamate receptor 2	0.0044	−0.2747	**0.0102**	**−0.5101**	**0.004**	−2.402
Crym	Mu-crystallin homolog	0.0065	−0.2962	**0.0292**	**−0.6153**	0.161	−0.897
Nr4a1	Nuclear receptor subfamily 4, group A, member 1	0.0074	−0.2802	**0.0063**	**−0.7108**	**0.001**	−2.402
Nr4a3	Nuclear receptor subfamily 4, group A, member 3	0.0061	−0.3224	**0.0005**	**−1.2155**	Nondetectable	
Slc1a3	Glial high affinity glutamate transporter	0.7954	−0.0163	Not assessed		Nondetectable	

Validation of selected genes determined to be differentially expressed in the mPFC exposed group ($n = 9$) versus control ($n = 9$) by microarray analysis or in the IL of the exposed group ($n = 5$) versus control ($n = 5$) is shown. Bold values are confirmed qRT-PCR data from microarray results. FC, fold change.

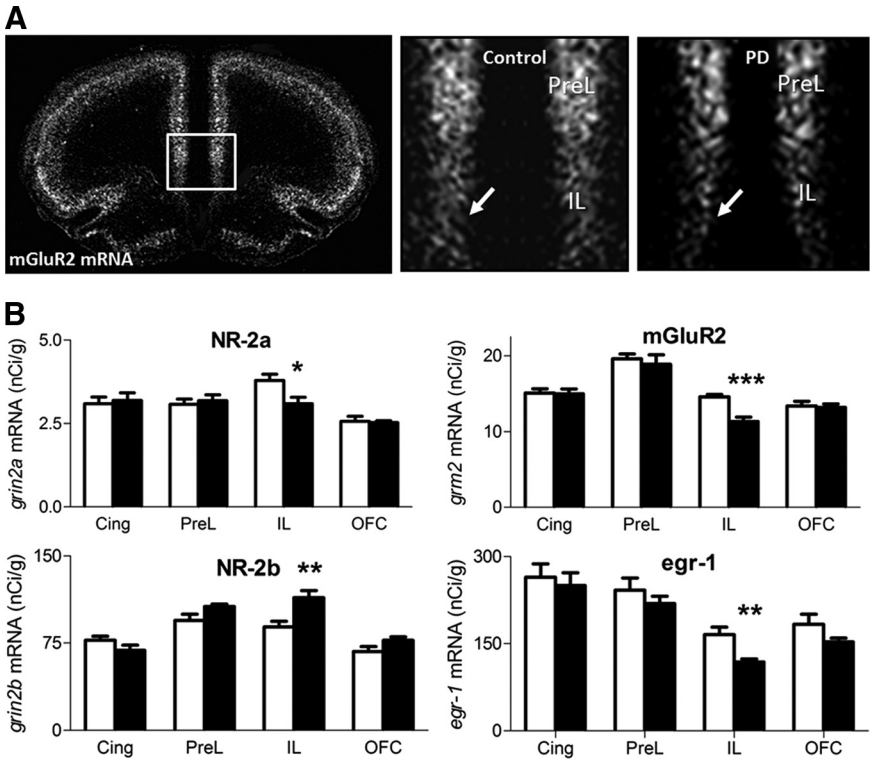

Figure 2. Prefrontal *in situ* hybridization point to the infralimbic cortex as major site of neuroadaptations. ***A***, Dark-field microphotographs from autoradiograms of *in situ* hybridization of *Grm2* from control and postdependent (PD) rats on coronal sections, +2.2 mm relative to bregma level. Enlarged images for both groups on the right. Arrows indicate signal in the infralimbic region. ***B***, Quantification of *in situ* expression levels (nanocuries per gram, mean ± SEM) in postdependent (black bars) versus control rats (white bars) for selected candidate genes significantly altered. *Nr-2a*, *Nr-2b*, *Egr1*, and *Grm2* mRNAs are robustly altered within the infralimbic cortex, but unaffected in cingulate, prelimbic, or orbitofrontal cortex. $^*p < 0.05$; $^{**}p < 0.01$; $^{***}p < 0.001$ comparing postdependent versus control (Student's *t* test). Cing, Cingulate cortex; PreL, prelimbic cortex; IL, infralimbic cortex; OFC, orbitofrontal cortex.

circuitry involved, we used a strategy that allows labeling pyramidal neurons within the infralimbic cortex via their projections to the nucleus accumbens shell subregion. We performed retrograde tracing by infusing rhodamine-labeled fluorescent latex microspheres into the nucleus accumbens shell (Katz and Iarovici, 1990; Reynolds and Zahm, 2005), isolated the labeled cell population (~70–100 cells) within the infralimbic cortex through LCM, and extracted the RNA for expression analysis (Fig. 3*A*,*B*).

We tested eight candidate genes from the mPFC microarray experiment (Table 3). Among these, *Grm2* as well as the Egr-family genes *Egr2* and *Egr4* were identified as significantly downregulated in the infralimbic cortex neurons of the postdependent group. Expression differences detected within the purified neuronal population were markedly enhanced compared to those in the analysis performed on tissue homogenates. Expression of *Grm2* and *Egr2* was ~10-fold and ~500-fold, respectively, altered in enriched infralimbic projection neuron populations from postdependent rats (Fig. 3*C*), although these differences were less than twofold when applying the same PCR analysis to tissue homogenates. The experiment reveals the extent to which major dysregulation can be disguised in heterogeneous samples and emphasizes the importance of studying well-characterized cell populations in the brain. In conclusion, we demonstrate that infralimbic–accumbal glutamatergic projection neurons are highly sensitive to alcohol dependence-induced neuroadaptations, and identify mGluR$_2$ receptor downregulation in this pathway as a candidate mechanism for observed behavioral deficits.

Functional consequences of mGluR$_2$ reduction

mGluR$_2$ function in the corticoaccumbal pathway was assessed by *in vivo* microdialysis. We measured extracellular glutamate levels in the nucleus accumbens shell of freely moving rats (Fig. 4*A*). Given its role as a presynaptic autoreceptor, stimulation of mGluR$_2$ is expected to downregulate glutamate release, resulting in reduced glutamate overflow in the dialysate. Accordingly, systemic administration of the mGluR$_{2/3}$ agonist LY379268 (3 mg/kg, i.p.) resulted in a robust and sustained decrease of extracellular glutamate levels in the nucleus accumbens shell of control rats. In contrast, no such effect was seen in postdependent rats (Fig. 4*B*). Basal glutamate levels were not different between postdependent and control rats (Fig. 4*B*). These data are consistent with the interpretation that the downregulation of *Grm2* expression could lead to a lack of mGluR$_2$ autoreceptor function at the terminals of the infralimbic projection neurons. Such a deficit would impact on activity-dependent glutamatergic neurotransmission in the corticostriatal pathway and presumably also on behavioral output.

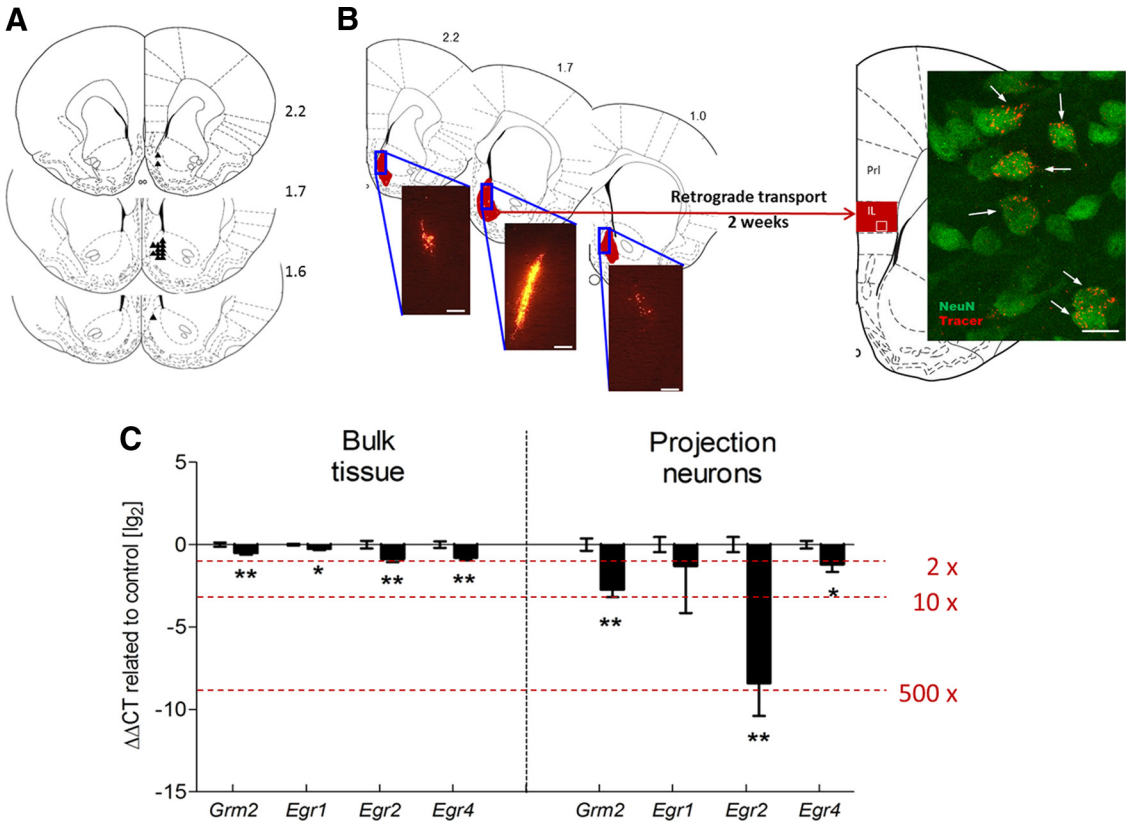

Figure 3. Robust downregulation of *Grm2* transcripts in rat infralimbic accumbens shell projection neurons lead to blunted response to *Grm2* agonist treatment in postdependent (PD) rats. ***A***, Locations of the 33 gauge injection cannula tips for the injections the retrograde tracer into the nucleus accumbens shell are represented by small black triangles. The cannula placements for the nucleus accumbens shell were verified within the region from +1.6 to +2.2 mm. ***B***, Distribution of retrograde tracer within the nucleus accumbens shell (range, +2.2 to +1.0 mm relative to bregma). Fluorescent cells were clearly visible in sections from +1.9 to +2.5 mm relative to bregma in the infralimbic and the dorsal peduncular cortex. Insert shows a representative confocal microscope image. Arrows indicate retrograde tracer-positive cells, colabeled with the neuronal marker NeuN. Scale bars: left, 100 μm; right, 10 μm. ***C***, Downregulated genes in glutamatergic projection neurons in the infralimbic cortex compared to the micropunched mPFC (bulk tissue) from the microarray study. The graph represents the delta delta cycle threshold ± SEM on a logarithmic scale of selected mRNAs, expressing the change in cycle thresholds from treatment to controls compared back to an endogenous control. In addition, *Crym*, a marker gene of glutamatergic pyramidal neurons according to the GENSAT mouse brain atlas (www.gensat.org), was highly expressed in all samples (quantitative PCR cycle threshold of ~14), whereas *Slc1a3*, the gene for the glial glutamate transporter, was not detectable (cycle threshold, >39), indicating that we indeed succeeded in collecting a highly purified glutamatergic neuronal population. *$p <$ 0.05; **$p <$ 0.01. PreL, Prelimbic cortex; IL, infralimbic cortex.

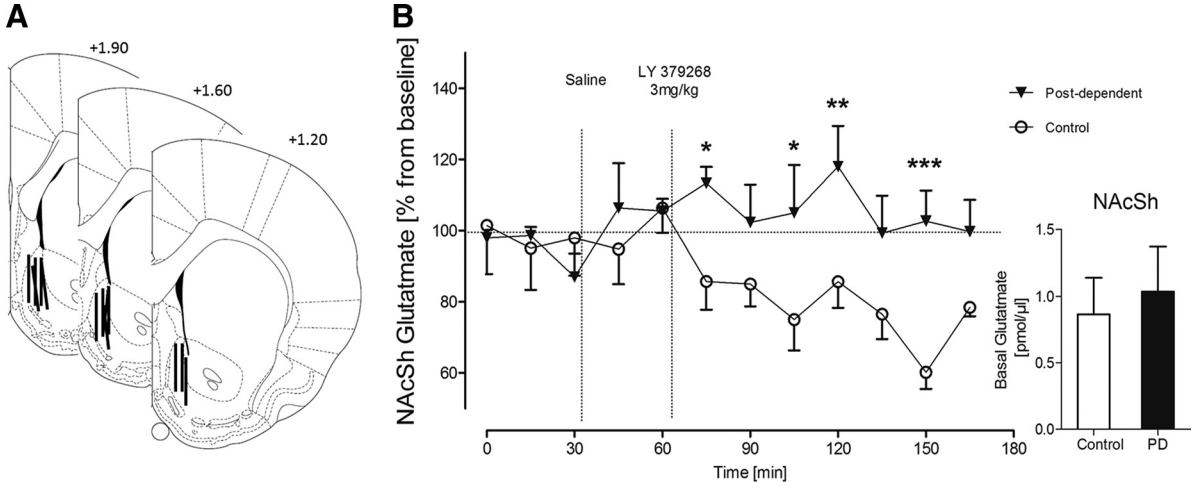

Figure 4. Glutamate microdialysis in postdependent (PD) versus control animals shows blunted response to mGluR$_2$ agonist treatment in postdependent rats. ***A***, The active membranes of the microdialysis probes are represented by black lines and were verified within the nucleus accumbens shell from +1.9 to +1.2 anterior to bregma. ***B***, Nucleus accumbens shell glutamate levels after intraperitoneal application of 3 mg/kg mGluR$_{2/3}$ agonist LY379268. Control animals show decrease of extracellular glutamate levels, whereas postdependent rats show a blunted response to the agonist treatment, indicating a downregulation of mGluR$_2$. Inset, Basal glutamate levels (two-way ANOVA; main effect of ethanol dependence history, $F_{(1,11)} = 6.672$, $p < 0.05$; main effect of time, $F_{(11,121)} = 1.521$, not significant; significant interaction of ethanol dependence history by time, $F_{(11,121)} = 2.331$, $p < 0.05$). *$p < 0.05$; **$p < 0.01$; ***$p < 0.001$ (Fisher LSD *post hoc* test). NAcSh, Nucleus accumbens shell.

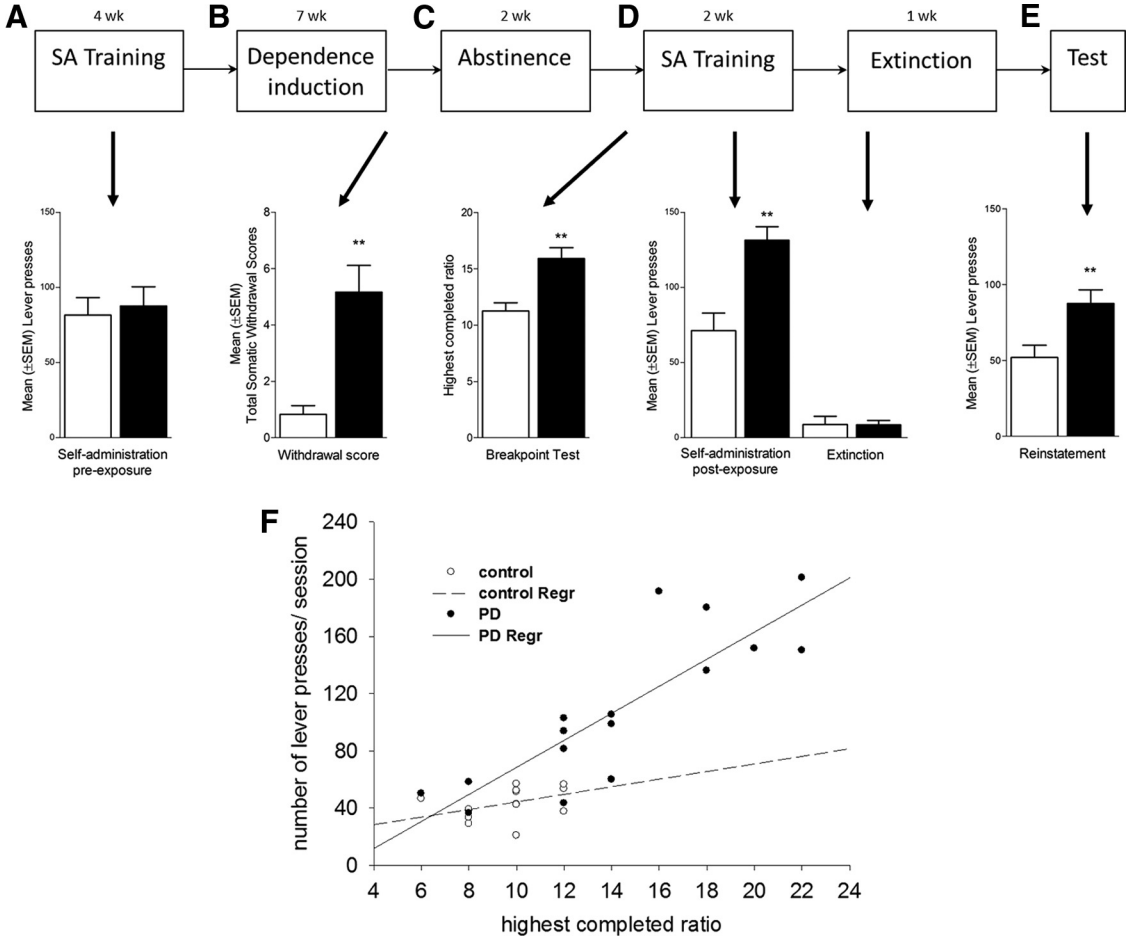

Figure 5. Diagram illustrating the experimental procedure of the postdependent (PD) cue-induced reinstatement model. ***A***, Animals underwent alcohol self-administration under a fixed ratio FR1 schedule until they reached stable lever presses accompanied by discrete cues predicting alcohol availability (CS+). Control and postdependent rats do not differ in this phase. After initial training, half of the animals (resulting in the postdependent group) were alcohol vapor exposed for 7 weeks. ***B***, At the end of the 7 week exposure, withdrawal signs were scored 8 h after last intoxication. Following 2 weeks of abstinence, rats were retrained to self-administer alcohol. ***C***, ***D***, Postdependent rats show higher self-administration (***D***) and also higher motivation (***C***) for alcohol in a progressive ratio test. Two-way ANOVA showed a significant main effects of ethanol dependence history ($F_{(1,24)} = 8.91$, $p < 0.01$) and significant interactions of ethanol dependence history by self-administration condition ($F_{(1,92)} = 6.08$, $p < 0.05$). Extinction training was not different between groups (postdependent vs control groups, $t_{(30)} = 0.243$, not significant). ***E***, Presentation of the CS+ elicits in significant reinstatement in control and postdependent rats with significant higher levels in the postdependent group (control, 42.1 ± 3.4 vs postdependent, 84.4 ± 13.2; $t_{(13)} = -2.896$, $p < 0.01$). ***F***, Linear regression analysis of mean lever presses and performance in the progressive ratio test of postdependent and control rats. Both groups show a significant deviation from zero (postdependent, $p = 0.004$; control, $p = 0.009$). Furthermore, postdependent rats show a significantly steeper slope of the correlation between response rates during ethanol self-administration under an FR1 schedule, and progressive ratio breakpoints. Error bars indicate SEM.

Restoration of mGluR$_2$ attenuates excessive cue-induced alcohol seeking

We next examined the role of mGluR$_2$ receptors in infralimbic neurons projecting to the nucleus accumbens shell for cue-induced reinstatement of alcohol-seeking behavior, an established animal model of relapse (Epstein et al., 2006; Sanchis-Segura and Spanagel, 2006). First, rats were trained to self-administer alcohol before alcohol vapor exposure (Fig. 5*A–E*). After the last exposure cycle, postdependent rats showed clear signs of withdrawal (approximately five of a maximal eight points from a global withdrawal score) (Macey et al., 1996), whereas this rating for control rats was close to zero ($p < 0.004$, Mann–Whitney; Fig. 5*B*). After 2 weeks of recovery, all rats were retrained to self-administer ethanol until stable response rates were achieved once more. Control rats regained self-administration rates that were similar to their preexposure rates (90% of preexposure). In contrast, postdependent rats rapidly escalated their self-administration rates by >155% (Fig. 5*A*,*D*). Motivation to obtain alcohol was further assessed by a progressive ratio reinforcement schedule (Hodos, 1961). Postdependent rats showed a significantly higher break point for alcohol self-administration than controls ($t_{(29)} = 3.09$, $p < 0.01$; Fig. 5*C*), a significantly steeper slope of the correlation between response rates during ethanol self-administration under an FR1 schedule, and progressive ratio breakpoints (correlation equations test, $p < 0.05$; Fig. 5*F*). This shows that escalated alcohol self-administration in postdependent rats is associated with an increased motivation to obtain the drug reinforcer, a key characteristic of addictive behavior (Deroche-Gamonet et al., 2004). These data are consistent with a recent report that also showed increased motivation to obtain ethanol following a history of experimenter imposed alcohol dependence (Kufahl et al., 2011; Vendruscolo et al., 2012).

Alcohol associated cues are potent triggers of relapse in alcoholic patients. This pathological behavior is typically modeled in the reinstatement procedure (Epstein et al., 2006; Sanchis-Segura and Spanagel, 2006). Following stable lever responding accompanied by discrete cues predicting alcohol availability (CS+), postdependent and control rats underwent extinction (Fig. 5*D*)

followed by a cue-induced reinstatement test. Postdependent rats displayed significantly higher reinstatement of alcohol seeking than control rats ($p < 0.01$; Fig. 5*E*). To directly assess the role of $mGluR_2$ in mPFC for cue-induced reinstatement of alcohol seeking, we generated two lentiviral vectors expressing either the $mGluR_2$ receptor together with eGFP or eGFP alone (lenti-$mGluR_2$ and lenti-control, respectively; Fig. 6*A*). Following alcohol/cue training, all rats went through extinction training, resulting in fewer than 10 responses (Fig. 6*F*). After completion of extinction training, rats were bilaterally injected with the respective lentiviral constructs into the infralimbic cortex (Fig. 6*B–F*), allowed to recover, and examined for cue-induced reinstatement of alcohol seeking. Notably, immunohistochemistry confirmed the coexpression of the lenti-$mGluR_2$ construct for all studied animals exclusively in the infralimbic cortex and in their neuronal projection target, the nucleus accumbens shell, EGFP-positive axon terminals were clearly visible (Fig. 6*D*,*E*). Presentation of the ethanol-associated cues resulted in significant resumption of operant responding in animals receiving the control lentiviral construct (paired *t* test; control, $t_{(7)} = 4.157$, $p < 0.01$; postdependent, $t_{(7)} = 4.211$, $p < 0.01$; Fig. 6*F*), with a highly increased mean (±SEM) number of responses in postdependent (87.6 ± 8.9) compared to control (51.9 ± 8.1) rats. Lenti-$mGluR_2$ did not significantly alter drug-seeking behavior in controls. However, lenti-$mGluR_2$ showed significant reduction in postdependent animals, such that their lever-pressing behavior declined for ~40% to control levels. These effects were confirmed by two-way ANOVA with significant main effects of ethanol dependence history ($F_{(1,24)} = 9.947$, $p < 0.01$) and virus treatment ($F_{(1,24)} = 7.932$, $p < 0.01$), but no significant interaction ($F_{(1,43)} = 2.032$, $p = 0.163$). We did not find time-dependent spontaneous recovery of lever pressing when reexposing the animals to the operant chamber after the 1 week time delay between the last extinction trial followed by sham operation and the reinstatement test (extinction, 8.9 ± 1.3; spontaneous recovery, 10.9 ± 2.5, not significant). We also did not find evidence for behavioral abnormalities (for example, weight loss, agitation, and self-injury) in any experimental group. Lenti-control and lenti-$mGluR_2$ rats did not differ in locomotor activity or their responding for natural rewards under the same reinforcement schedule used for ethanol self-administration (Fig. 7*A–C*), demonstrating that effects of $mGluR_2$ overexpression on reduced ethanol-seeking behavior were not secondary to alterations in task performance.

Downregulated GRM2 in human alcoholics

To translate these animal findings to humans, we determined GRM2 expression in postmortem brain tissue samples from alcohol-dependent patients and controls matched for age and postmortem interval (Sheedy et al., 2008).

A human brain region that is anatomically and functionally related to the rodent mPFC is the anterior cingulated cortex (Uylings et al., 2003). However, it has to be pointed out that a one-to-one relationship between human and rodent prefrontocortical regions does not exist and functional elements of rodent distinctions including of the infralimbic cortex can be found in various areas of the enlarged human prefrontocortical volume. Within the anterior cingulate cortex, we found a significant, 2.6-fold decrease in GRM2 transcript levels in alcoholics compared to controls (Fig. 8*A*,*B*).

Discussion

The data presented here provide a fundamentally new insight into the molecular basis by which a prolonged history of alcohol dependence causes a substantial and long-lasting reorganization of the medial prefrontal cortex. To the best of our knowledge, the present data from gene expression and functional studies constitute strong experimental evidence of anatomical and molecular pathway-specific plasticity in the mPFC as a sequel to alcohol dependence and establish a key pathophysiological mechanism for the increased propensity to relapse. In particular, we discovered a locally restricted but profound molecular pathology, namely, the infralimbic cortex-specific expression deficit of $mGluR_2$, as a critical component for excessive alcohol seeking in postdependent rats, and that restoring this receptor function is sufficient for regaining control over this addictive behavior.

The infralimbic cortex shows a unique pattern of alcohol dependence-induced alterations, as evidenced by the regional-specific downregulation of transcription factors *Egr1* and *Egr2* known to be involved in neuronal plasticity, as well as on the glutamate receptor genes *Grin2a*, *Grin2b*, and *Grm2*. Importantly, the downregulation of *Grm2* and *Egr2* is much more pronounced in purified infralimbic–accumbens shell projection neurons, ~10-fold and ~500-fold, respectively, highlighting these genes within this cell population as functionally relevant for the pathological process. Notably, the *Grm2* promoter contains transcription factor binding sites for the *Egr*-family as well as a unique *Egr2* binding site (according to the DECODE database, http://www.sabiosciences.com/chipqpcrsearch.php?app=TFBS), which provide a potential substrate for regulation of *Grm2* expression by *Egr2*. On the other hand, $mGluR_2$ may regulate *Egr2* expression, as suggested by experiments in *Grm2* knock-out mice that show a lack of *Egr2* activation following drug application (Moreno et al., 2011). Whether or not the downregulation of these genes is functionally related is yet unknown, but both seem to be involved in dependence-related plasticity of glutamatergic neurons, $mGluR_2$ directly at the level of the synapse, and *Egr2* via stimulus-transcription coupling.

Importantly, we found a lack of $mGluR_2$ receptor function in the terminal fields of the infralimbic projections, which became evident as an inability of these neurons to modulate nucleus accumbens shell glutamate levels in response to receptor stimulation with an $mGluR_{2/3}$ agonist. This effect is consistent with the pronounced reduction in $mGluR_2$ expression—with no change in $mGluR_3$ expression—in the infralimbic cortex of postdependent rats. However, a recent study found no differences in $mGluR_{2/3}$ functional activity within the mPFC in postdependent rats after 4 weeks of repeated cycles of vapor exposure (Kufahl et al., 2011). How can this discrepancy been explained? We demonstrated previously that in the alcohol vapor exposure procedure, a temporal threshold for induction of escalation of alcohol consumption and concomitant neuroplastic changes occur (Rimondini et al., 2003). Hence, postdependent rats that were exposed to alcohol vapor for 7 weeks displayed a marked increase in alcohol self-administration, whereas postdependent rats exposed for shorter periods (2 and 4 weeks) did not show such an escalation (Rimondini et al., 2003). Here we report that postdependent rats exposed to alcohol vapor for 7 weeks show an augmented reinstatement response of alcohol-seeking behavior and that this dependence-like phenotype is directly linked to an $mGluR_2$ deficit in the infralimbic cortex. In the study by Kufahl et al. (2011), rats were exposed to alcohol vapor for 4 weeks and did not differ either in their reinstatement response nor in $mGluR_{2/3}$ functional

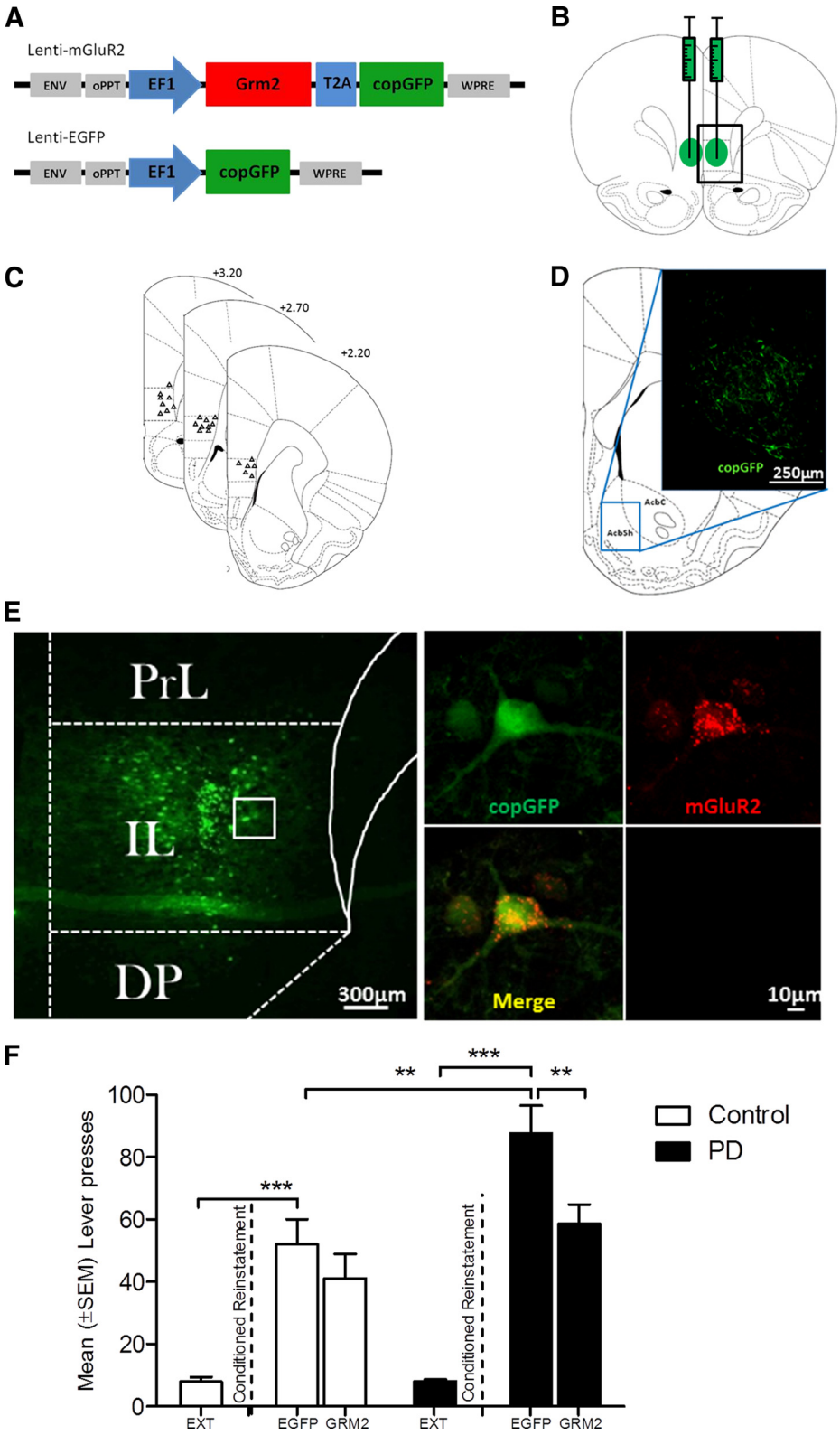

Figure 6. Conditioned reinstatement of drug-seeking behavior attenuates only with lenti-mGluR$_2$ bilateral viral injections. ***A***, Schematic representation of the lentiviral expression plasmids used for the production of Lenti-mGluR$_2$ and Lenti-EGFP. cPPT, central polypurine tract; copGFP, copepod Pontellina plumata GFP; WPRE, Woodchuck Hepatitis Virus Posttranscriptional Regulatory Element. ***B***, Illustration of bilateral Lenti-mGluR$_2$ and Lenti-EGFP injection sites. Green circles represent the spread area of the virus. ***C***, Locations of the 33 gauge injection cannula tips for the lentiviral injection into the infralimbic cortex are represented by small black triangles, respectively. The cannula placements were verified within the infralimbic cortex from +3.2 to +2.2 anterior to bregma. ***D***, Schematic representation of the infralimbic projection site. The inset shows the nucleus accumbens shell region with its EGFP positive axons originating from the injection site at 7 d after lentiviral infection. ***E***, Left, Site of Lenti-mGluR$_2$ delivery adapted from Paxinos and Watson's (1998) rat brain atlas. Right, Representative microscope image of a virally infected cell in the infralimbic cortex showing mGluR$_2$, EGFP, merged and secondary antibody negative control. EGFP and mGluR$_2$ expression was assessed using immunohistochemistry. PrL, Prelimbic cortex; IL, infralimbic cortex; DP, dorsal peduncular cortex. ***F***, Presentation of the CS+ elicits in significant reinstatement in both control and PD rats with lenti-EGFP. Lenti-mGluR$_2$ significantly attenuates drug-seeking behavior only in postdependent (PD) rats down to the level of the control group. $^*p < 0.05$; $^{**}p < 0.01$; $^{***}p < 0.001$. For detailed statistics, see Results. Error bars indicate SEM.

activity from controls, which supports the definition of a temporal threshold for induction of escalation in alcohol consumption and alcohol seeking and the herewith associated neuroplastic changes. Together, a careful, cell type-specific investigation of the group II mGluRs shows a highly restricted mGluR$_2$ downregulation in sparsely distributed glutamatergic neurons located in the ventral part of the mPFC, the infralimbic region.

With our viral rescue experiment, we could further show that mGluR$_2$ receptors in infralimbic neurons are necessary for the control exerted by this region on alcohol seeking. Consequently, infralimbic neurons in postdependent animals are capable of eliciting a sufficient glutamate response to drug cues, but in the absence of feedback provided by mGluR$_2$ receptors, the information transmitted by this signal cannot be properly processed, thereby disrupting adequate behavioral control. On the other hand, adding extra mGluR$_2$ autoreceptors to normal infralimbic neurons does not seem to disrupt glutamatergic signaling and behavioral output in a task controlled by this brain structure. This concept is further supported by electrophysiological evidence from long-term cocaine-exposed rats., Using *in vivo* stimulation from the prefrontal cortex of long-term cocaine-exposed rats revealed an mGluR$_{2/3}$ deficit in the nucleus accumbens (Moussawi et al., 2011). In another model of cocaine-induced addiction-like behavior, there was a lack in mGluR$_{2/3}$-mediated long-term depression in mPFC neurons that was associated with a strong downregulation of mGluR$_{2/3}$ receptors (Kasanetz et al., 2012). Thus, both alcohol and cocaine dependence are associated with medioprefrontal mGluR$_2$ deficits that may lead to an inflexible state of the brain. Although we did not provide electrophysiological evidence, our study substantially extends the findings from the cocaine models by demonstrating that an addiction-like behavior, here excessive alcohol seeking, can be rescued through restoring mGluR$_2$ levels in the mPFC.

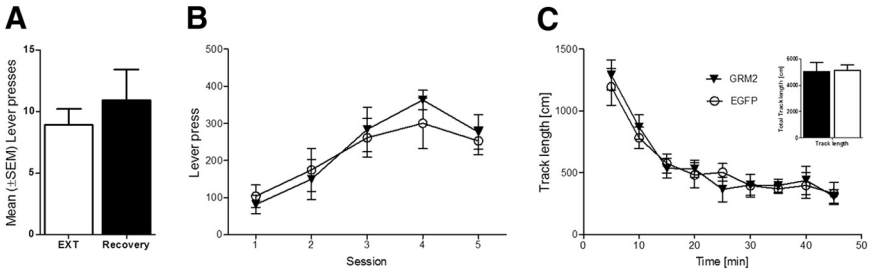

Figure 7. Behavioral observations for the delayed reinstatement and between Lenti-mGluR$_2$- and Lenti-EGFP-injected animals in responding for natural rewards and in locomotor activity. ***A***, We did not find time-dependent spontaneous recovery of lever pressing when reexposing the animals to the operant chamber after the 1 week time delay between last extinction trial followed by sham operation and reinstatement test. No differences were observed between Lenti-mGluR$_2$- and Lenti-EGFP-injected animals in responding for natural rewards and in locomotor activity. ***B***, Both groups were exposed to five 30 min operant sessions to self-administered sweetened condensed milk under an FR1 schedule. Lenti-mGluR$_2$ and Lenti-EGFP lever-pressing behavior did not differ. ***C***, Lenti-mGluR$_2$ and Lenti-EGFP rats show equal locomotion when exposed to a 45 min open-field session. Inset, Total track length completed in the 45 min session. Error bars indicate SEM.

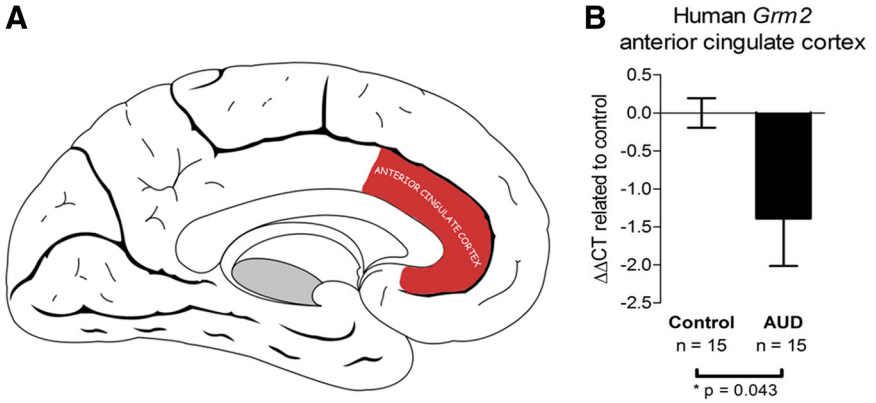

Figure 8. Downregulation of *Grm2* transcript in the human anterior cingulated cortex. ***A***, Schematic representation of the anterior cingulate cortex of the human brain on a sagittal section (adapted from Standring, 2008). ***B***, RT-qPCR showing *Grm2* downregulation in the human anterior cingulate cortex of patients classified with alcohol use disorder compared to respective controls. $*p < 0.05$ (Student's *t* test). Error bars indicate SEM. AUD, alcohol use disorder.

Impairments in executive control over behavior are known risk factors for drug addiction (Everitt and Robbins, 2005). Alcohol-dependent patients have severe deficits in many aspects of prefrontocortical functions encompassing emotion, cognition, and behavior, whereby medial subdivisions of the prefrontal cortex are of particular interest here because of their role in motivation, control of emotions, salience attribution, and decision making (Goldstein and Volkow, 2011). These functions have been established not only in humans but also in rodents (Uylings et al., 2003). Typical behaviors seen in patients with damage to the ventromedial PFC are social inappropriateness, impulsivity, and poor judgment (Bechara et al., 1994). Enduring medioprefrontal gray matter losses were found in alcoholic patients and are associated with severe functional deficits in the ability to control reward-predicting stimuli (Duka et al., 2011). Interestingly, these deficits increase with the number of detoxifications experienced by the patients, which resonates with previous observations in experimental animals that the number of withdrawals, rather than the mere level of intoxication, is important for the occurrence of long-lasting behavioral and neural symptoms, i.e., a postdependent state (Roberts et al., 2000; Stephens et al., 2005; Sommer et al., 2008; Heilig et al., 2010). A previous fMRI study in alcoholics found increased mPFC activation in response to alcohol cues, which was positively correlated with relapse risk (Grüsser et al., 2004). In experimental animals, cue presentation of conditioned stimuli predicting a drug reward results in a significant increase in glutamate levels in the nucleus accumbens (Hotsenpiller et al., 2001). Most likely, this input derives from prefrontal areas, given that the mPFC–accumbal glutamatergic pathway is necessary for reinstating drug-seeking behavior. Likewise, our observed deficit in mGluR$_2$ autoreceptor function within the infralimbic cortex of postdependent rats may lead to increased accumbal glutamate levels after cue presentation, with subsequent excessive drug-seeking behavior.

Importantly, we also find a reduction in GRM2 expression in the anterior cingulate cortex from alcohol-dependent patients, which suggests that the deficits found in our animal model may be a feature in alcoholism in at least some patients. It remains to be clarified whether or not the reduced GRM2 expression found in the present sample is functionally linked to the progressive reduction in prefrontal neuronal density, which was seen in a previous study on postmortem brain tissue from alcoholics

(Miguel-Hidalgo et al., 2006). However, the reduction in GRM2 expression and number of neurons may together lead to an absolute deficit of $mGluR_2$ receptors in the mPFC of alcoholics. This may have important implications for the development of treatments for relapse prevention because absolute deficits cannot be efficiently targeted by agonist treatment. Indeed, this may be one of the reasons for the relatively narrow therapeutic window for reducing alcohol seeking in experimental animals by $mGluR_{2/3}$ agonists (Kufahl et al., 2011). Thus, instead of focusing on the development of more specific $mGluR_2$ ligands, novel therapeutic strategies should attempt to overcome the blockade of $mGluR_2$ expression. Focal virus-mediated gene therapy, although potentially feasible (Kaplitt et al., 2007), is unlikely to be applied for the treatment of addictions. Alternatively, pharmacological approaches targeting key proteins involved in glutamate homeostasis, such as glutamate transporters or mGluRs, could potentially be effective treatments in relapse prevention. In conclusion, the present study illustrates the feasibility of a structured discovery strategy, that starting with an unbiased screening over progressively narrowing experimental approaches allows identifying a specific pathological mechanism and can point toward new directions for therapeutic development.

References

American Psychiatric Association (1994) Diagnostic and statistical manual of mental health disorders, 4th ed. Washington, DC: American Psychiatric Association.

Arlinde C, Sommer W, Björk K, Reimers M, Hyytiä P, Kiianmaa K, Heilig M (2004) A cluster of differentially expressed signal transduction genes identified by microarray analysis in a rat genetic model of alcoholism. Pharmacogenomics J 4:208–218. CrossRef Medline

Bechara A, Damasio AR, Damasio H, Anderson SW (1994) Insensitivity to future consequences following damage to human prefrontal cortex. Cognition 50:7–15. CrossRef Medline

Becker HC, Lopez MF (2004) Increased ethanol drinking after repeated chronic ethanol exposure and withdrawal experience in C57BL/6 mice. Alcohol Clin Exp Res 28:1829–1838. CrossRef Medline

Björk K, Hansson AC, Sommer WH (2010) Genetic variation and brain gene expression in rodent models of alcoholism implications for medication development. Int Rev Neurobiol 91:129–171. CrossRef Medline

Capriles N, Rodaros D, Sorge RE, Stewart J (2003) A role for the prefrontal cortex in stress- and cocaine-induced reinstatement of cocaine seeking in rats. Psychopharmacology (Berl) 168:66–74. CrossRef

Ciccocioppo R, Martin-Fardon R, Weiss F (2002) Effect of selective blockade of mu(1) or delta opioid receptors on reinstatement of alcohol-seeking behavior by drug-associated stimuli in rats. Neuropsychopharmacology 27:391–399. CrossRef Medline

Cornish JL, Kalivas PW (2000) Glutamate transmission in the nucleus accumbens mediates relapse in cocaine addiction. J Neurosci 20:RC89. Medline

Deroche-Gamonet V, Belin D, Piazza PV (2004) Evidence for addiction-like behavior in the rat. Science 305:1014–1017. CrossRef Medline

Duka T, Trick L, Nikolaou K, Gray MA, Kempton MJ, Williams H, Williams SC, Critchley HD, Stephens DN (2011) Unique brain areas associated with abstinence control are damaged in multiply detoxified alcoholics. Biol Psychiatry 70:545–552. CrossRef Medline

Epstein DH, Preston KL, Stewart J, Shaham Y (2006) Toward a model of drug relapse: an assessment of the validity of the reinstatement procedure. Psychopharmacology (Berl) 189:1–16. CrossRef

Everitt BJ, Robbins TW (2005) Neural systems of reinforcement for drug addiction: from actions to habits to compulsion. Nat Neurosci 8:1481–1489. CrossRef Medline

Ferraguti F, Shigemoto R (2006) Metabotropic glutamate receptors. Cell Tissue Res 326:483–504. CrossRef Medline

Funk CK, O'Dell LE, Crawford EF, Koob GF (2006) Corticotropin-releasing factor within the central nucleus of the amygdala mediates enhanced ethanol self-administration in withdrawn, ethanol-dependent rats. J Neurosci 26:11324–11332. CrossRef Medline

Goldstein RZ, Volkow ND (2011) Dysfunction of the prefrontal cortex in addiction: neuroimaging findings and clinical implications. Nat Rev Neurosci 12:652–669. CrossRef Medline

Gray H (1918) Anatomy: descriptive and surgical.

Grüsser SM, Wrase J, Klein S, Hermann D, Smolka MN, Ruf M, Weber-Fahr W, Flor H, Mann K, Braus DF, others (2004) Cue-induced activation of the striatum and medial prefrontal cortex is associated with subsequent relapse in abstinent alcoholics. Psychopharmacology (Berl) 175:296–302. CrossRef

Hansson AC, Rimondini R, Neznanova O, Sommer WH, Heilig M (2008) Neuroplasticity in brain reward circuitry following a history of ethanol dependence. Eur J Neurosci 27:1912–1922. CrossRef Medline

Heilig M, Koob GF (2007) A key role for corticotropin-releasing factor in alcohol dependence. Trends Neurosci 30:399–406. CrossRef Medline

Heilig M, Egli M, Crabbe JC, Becker HC (2010) Acute withdrawal, protracted abstinence and negative affect in alcoholism: are they linked? Addict Biol 15:169–184. CrossRef Medline

Hermann D, Weber-Fahr W, Sartorius A, Hoerst M, Frischknecht U, Tunc-Skarka N, Perreau-Lenz S, Hansson AC, Krumm B, Kiefer F, Spanagel R, Mann K, Ende G, Sommer WH (2012a) Translational magnetic resonance spectroscopy reveals excessive central glutamate levels during alcohol withdrawal in humans and rats. Biol Psychiatry 71:1015–1021. Medline

Hermann D, Frischknecht U, Heinrich M, Hoerst M, Vollmert C, Vollstädt-Klein S, Tunc-Skarka N, Kiefer F, Mann K, Ende G (2012b) MR spectroscopy in opiate maintenance therapy: association of glutamate with the number of previous withdrawals in the anterior cingulate cortex. Addict Biol 17:659–667. CrossRef Medline

Hodos W (1961) Progressive ratio as a measure of reward strength. Science 134:943–944. CrossRef Medline

Hotsenpiller G, Giorgetti M, Wolf ME (2001) Alterations in behaviour and glutamate transmission following presentation of stimuli previously associated with cocaine exposure. Eur J Neurosci 14:1843–1855. CrossRef Medline

Kalivas PW (2009) The glutamate homeostasis hypothesis of addiction. Nat Rev Neurosci 10:561–572. CrossRef Medline

Kaplitt MG, Feigin A, Tang C, Fitzsimons HL, Mattis P, Lawlor PA, Bland RJ, Young D, Strybing K, Eidelberg D, During MJ (2007) Safety and tolerability of gene therapy with an adeno-associated virus (AAV) borne GAD gene for Parkinson's disease: an open label, phase I trial. Lancet 369:2097–2105. CrossRef Medline

Kasanetz F, Lafourcade M, Deroche-Gamonet V, Revest JM, Berson N, Balado E, Fiancette JF, Renault P, Piazza PV, Manzoni OJ (2012) Prefrontal synaptic markers of cocaine addiction-like behavior in rats. Mol Psychiatry. Advance online publication. doi:10.1038/mp.2012.59. CrossRef

Katz LC, Iarovici DM (1990) Green fluorescent latex microspheres: a new retrograde tracer. Neuroscience 34:511–520. CrossRef Medline

Koob GF, Volkow ND (2010) Neurocircuitry of addiction. Neuropsychopharmacology 35:217–238. Medline

Kufahl PR, Martin-Fardon R, Weiss F (2011) Enhanced sensitivity to attenuation of conditioned reinstatement by the mGluR(2/3) agonist LY379268 and increased functional activity of mGluR(2/3) in rats with a history of ethanol dependence. Neuropsychopharmacology 36:1–12. CrossRef Medline

Liechti ME, Markou A (2007) Metabotropic glutamate 2/3 receptor activation induced reward deficits but did not aggravate brain reward deficits associated with spontaneous nicotine withdrawal in rats. Biochem Pharmacol 74:1299–1307. CrossRef Medline

Macey DJ, Schulteis G, Heinrichs SC, Koob GF (1996) Time-dependent quantifiable withdrawal from ethanol in the rat: effect of method of dependence induction. Alcohol 13:163–170. CrossRef Medline

McFarland K, Davidge SB, Lapish CC, Kalivas PW (2004) Limbic and motor circuitry underlying footshock-induced reinstatement of cocaine-seeking behavior. J Neurosci 24:1551–1560. CrossRef Medline

Melendez RI, McGinty JF, Kalivas PW, Becker HC (2012) Brain region-specific gene expression changes after chronic intermittent ethanol exposure and early withdrawal in C57BL/6J mice. Addict Biol 17:351–364. CrossRef Medline

Miguel-Hidalgo JJ, Overholser JC, Meltzer HY, Stockmeier CA, Rajkowska G (2006) Reduced glial and neuronal packing density in the orbitofrontal cortex in alcohol dependence and its relationship with suicide and dura-

tion of alcohol dependence. Alcohol Clin Exp Res 30:1845–1855. CrossRef Medline

Moreno JL, Holloway T, Albizu L, Sealfon SC, González-Maeso J (2011) Metabotropic glutamate mGlu2 receptor is necessary for the pharmacological and behavioral effects induced by hallucinogenic 5-HT2A receptor agonists. Neurosci Lett 493:76–79. CrossRef Medline

Moussawi K, Pacchioni A, Moran M, Olive MF, Gass JT, Lavin A, Kalivas PW (2009) N-Acetylcysteine reverses cocaine-induced metaplasticity. Nat Neurosci 12:182–189. CrossRef Medline

Moussawi K, Zhou W, Shen H, Reichel CM, See RE, Carr DB, Kalivas PW (2011) Reversing cocaine-induced synaptic potentiation provides enduring protection from relapse. Proc Natl Acad Sci U S A 108:385–390. CrossRef Medline

O'Dell LE, Roberts AJ, Smith RT, Koob GF (2004) Enhanced alcohol self-administration after intermittent versus continuous alcohol vapor exposure. Alcohol Clin Exp Res 28:1676–1682. CrossRef Medline

Ohishi H, Shigemoto R, Nakanishi S, Mizuno N (1993) Distribution of the messenger RNA for a metabotropic glutamate receptor, mGluR2, in the central nervous system of the rat. Neuroscience 53:1009–1018. CrossRef Medline

Olive MF (2009) Metabotropic glutamate receptor ligands as potential therapeutics for addiction. Curr Drug Abuse Rev 2:83–98. CrossRef Medline

Paxinos G, Watson C (1998) The rat brain in stereotaxic coordinates. San Diego: Academic.

Reimers M, Heilig M, Sommer WH (2005) Gene discovery in neuropharmacological and behavioral studies using Affymetrix microarray data. Methods 37:219–228. CrossRef Medline

Reynolds SM, Zahm DS (2005) Specificity in the projections of prefrontal and insular cortex to ventral striatopallidum and the extended amygdala. J Neurosci 25:11757–11767. CrossRef Medline

Rimondini R, Arlinde C, Sommer W, Heilig M (2002) Long-lasting increase in voluntary ethanol consumption and transcriptional regulation in the rat brain after intermittent exposure to alcohol. FASEB J 16:27–35. CrossRef Medline

Rimondini R, Sommer W, Heilig M (2003) A temporal threshold for induction of persistent alcohol preference: behavioral evidence in a rat model of intermittent intoxication. J Stud Alcohol 64:445–449. Medline

Rimondini R, Sommer WH, Dall'Olio R, Heilig M (2008) Long-lasting tolerance to alcohol following a history of dependence. Addict Biol 13:26–30. CrossRef Medline

Roberts AJ, Heyser CJ, Cole M, Griffin P, Koob GF (2000) Excessive ethanol drinking following a history of dependence animal model of allostasis. Neuropsychopharmacology 22:581–594. CrossRef Medline

Rogers J, Wiener SG, Bloom FE (1979) Long-term ethanol administration methods for rats: advantages of inhalation over intubation or liquid diets. Behav Neural Biol 27:466–486. CrossRef Medline

Sanchis-Segura C, Spanagel R (2006) Behavioural assessment of drug reinforcement and addictive features in rodents: an overview. Addict Biol 11:2–38. CrossRef Medline

Schacht JP, Anton RF, Myrick H (2013) Functional neuroimaging studies of alcohol cue reactivity: a quantitative meta-analysis and systematic review. Addict Biol 18:121–133. CrossRef Medline

Sheedy D, Garrick T, Dedova I, Hunt C, Miller R, Sundqvist N, Harper C (2008) An Australian Brain Bank: a critical investment with a high return! Cell Tissue Bank 9:205–216.

Sommer WH, Rimondini R, Hansson AC, Hipskind PA, Gehlert DR, Barr CS, Heilig MA (2008) Upregulation of voluntary alcohol intake, behavioral sensitivity to stress, and amygdala crhr1 expression following a history of dependence. Biol Psychiatry 63:139–145. CrossRef Medline

Sommer WH, Lidström J, Sun H, Passer D, Eskay R, Parker SCJ, Witt SH, Zimmermann US, Nieratschker V, Rietschel M, Margulies EH, Palkovits M, Laucht M, Heilig M (2010) Human NPY promoter variation rs16147:T>C as a moderator of prefrontal NPY gene expression and negative affect. Human Mut 31:E1594–E1608. CrossRef

Spanagel R (2009) Alcoholism: a systems approach from molecular physiology to addictive behavior. Physiol Rev 89:649–705. CrossRef Medline

Spanagel R, Bartsch D, Brors B, Dahmen N, Deussing J, Eils R, Ende G, Gallinat J, Gebicke-Haerter P, Heinz A, Kiefer F, Jäger W, Mann K, Matthäus F, Nöthen M, Rietschel M, Sartorius A, Schütz G, Sommer WH, Sprengel R, et al. (2010) An integrated genome research network for studying the genetics of alcohol addiction. Addict Biol 15:369–379. CrossRef Medline

Standring S (2008) Gray's anatomy: the anatomical basis of clinical practice, Ed 40. New York: Churchill-Livingstone/Elsevier.

Stephens DN, Ripley TL, Borlikova G, Schubert M, Albrecht D, Hogarth L, Duka T (2005) Repeated ethanol exposure and withdrawal impairs human fear conditioning and depresses long-term potentiation in rat amygdala and hippocampus. Biol Psychiatry 58:392–400. CrossRef Medline

Subramanian A, Tamayo P, Mootha VK, Mukherjee S, Ebert BL, Gillette MA, Paulovich A, Pomeroy SL, Golub TR, Lander ES, Mesirov JP (2005) Gene set enrichment analysis: a knowledge-based approach for interpreting genome-wide expression profiles. Proc Natl Acad Sci U S A 102:15545–15550. CrossRef Medline

Sugino K, Hempel CM, Miller MN, Hattox AM, Shapiro P, Wu C, Huang ZJ, Nelson SB (2006) Molecular taxonomy of major neuronal classes in the adult mouse forebrain. Nat Neurosci 9:99–107. CrossRef Medline

Tolliver GA, Sadeghi KG, Samson HH (1988) Ethanol preference following the sucrose-fading initiation procedure. Alcohol 5:9–13. CrossRef Medline

Uylings HB, Groenewegen HJ, Kolb B (2003) Do rats have a prefrontal cortex? Behav Brain Res 146:3–17. CrossRef Medline

Vendruscolo LF, Barbier E, Schlosburg JE, Misra KK, Whitfield TW Jr, Logrip ML, Rivier C, Repunte-Canonigo V, Zorrilla EP, Sanna PP, Heilig M, Koob GF (2012) Corticosteroid-dependent plasticity mediates compulsive alcohol drinking in rats. J Neurosci 32:7563–7571. CrossRef Medline

Wilson SJ, Sayette MA, Fiez JA (2004) Prefrontal responses to drug cues: a neurocognitive analysis. Nat Neurosci 7:211–214. CrossRef Medline